RESEARCH PAPER

SYNTHESIS, SPECTRAL CHARACTERIZATION, AND ANTIMYCOBACTERIAL EVALUATION OF FLUORINATED QUINOLONE ANALOGUES AGAINST MYCOBACTERIUM TUBERCULOSIS H37RV STRAIN

Neha Ronald William[1], Vilas Sawale[2], Landge Dhananjay Ashok[3*], Nitin B Ghiware[4], Parjinder Kaur[5], Richa[6], Vinay Hiralal Singh[7], Akruti Arvind Pratap Singh[8]

[2]Associate Professor, Usha Dwarkadas Pathrikar Institute of Pharmacy, Dongargaon Kawad, Phulambri, Chatrapati Sambhaji Nager

[3*]Associate Professor, Adsul College of Pharmacy, Chas Ahilyanagar, Maharashtra

[4]Professor, Department of Pharmacology, Nanded Pharmacy College, Shyam Nagar, Nanded, Maharashtra. 431605

[5]School of Pharmaceutical Sciences, CGC University, Mohali, Punjab - 140307, India

[6]Amity Institute of Pharmacy, Amity University, Noida, Uttar Pradesh

[7]Konkan Gyanpeeth Karjat College of ASC, Karjat, Raigad, Maharashtra, India. 410201

[8]Oriental College of Pharmacy, Sanpada, Navi Mumbai, Maharashtra, India. 400075

***Corresponding author: Landge Dhananjay Ashok, Associate Professor, Adsul College of Pharmacy, Chas Ahilyanagar, Maharashtra**

Email: dhananjaylandge33@gmail.com

Received: 25th May, 2026; **Revised:** 6th June, 2026; **Accepted:** 8th June, 2026; **Available Online:** 09th June, 2026

ABSTRACT

The emergence of multidrug-resistant strains of Tuberculosis has created an urgent need for the development of novel antitubercular agents with improved therapeutic efficacy. In the present investigation, a series of novel fluorinated quinolone analogues were synthesized, spectrally characterized, and evaluated for their antimycobacterial activity against the H37Rv strain of Mycobacterium tuberculosis. The fluorinated quinolone derivatives were synthesized using the Gould–Jacobs cyclization approach followed by hydrolysis and recrystallization procedures. The synthesized compounds were characterized using FTIR, ^{1}H NMR, ^{13}C NMR, mass spectrometry, and elemental analysis for structural confirmation. Antimycobacterial activity was evaluated using the Microplate Alamar Blue Assay method, and minimum inhibitory concentration values were determined. The synthesized analogues demonstrated significant variation in antimycobacterial activity depending on the nature of aromatic substitution. Among all compounds, FQ-3 containing a trifluoromethylphenyl substituent exhibited the highest antimycobacterial activity with an MIC value of 0.25 µg/mL, followed by FQ-2 possessing a 3,4-difluorophenyl substitution with an MIC value of 0.5 µg/mL. Structure–activity relationship analysis indicated that electron-withdrawing fluorinated substituents markedly enhanced antimycobacterial potency. The study demonstrated that fluorinated quinolone analogues represent promising scaffolds for future antitubercular drug development and warrant further pharmacological and mechanistic investigations.

Keywords: Fluorinated quinolone analogues, antimycobacterial activity, H37Rv strain, Microplate Alamar Blue Assay, structure–activity relationship, medicinal chemistry, fluorinated heterocycles.

How to cite this article: William NR, Sawale V, Ashok LD, Ghiware NB, Kaur P, Richa, Singh VH, Singh AAP. Synthesis, Spectral Characterization, and Antimycobacterial Evaluation of Fluorinated Quinolone Analogues Against Mycobacterium Tuberculosis H37Rv Strain. Int J Drug Deliv Technol. 2026;16(57s): 1911-1920. DOI: 10.25258/ijddt.16.57s.194

Source of support: Nil.

Conflict of interest: None.

1. INTRODUCTION

Tuberculosis remains one of the most devastating infectious diseases worldwide and continues to represent a major global public health challenge. Despite substantial advances in chemotherapy and disease management, tuberculosis remains responsible for millions of new infections and deaths annually, particularly in developing and underdeveloped countries. The causative organism, *Mycobacterium tuberculosis*, is a slow-growing acid-fast bacillus possessing a highly complex lipid-rich cell wall that contributes significantly to its pathogenicity, persistence, and intrinsic resistance to several antimicrobial agents. The emergence of multidrug-resistant (MDR) and extensively drug-resistant (XDR) strains has further complicated tuberculosis treatment and reduced the efficacy of existing therapeutic regimens. Additionally, prolonged treatment duration, poor patient compliance, drug toxicity, and drug–drug interactions have intensified the urgent need for the development of novel antitubercular agents with improved safety and efficacy profiles (A *et al.*, 2025; Abayneh *et al.*, 2025; Abdjul *et al.*, 2025; Agnivesh *et al.*, 2025).

Among the various classes of antibacterial agents, quinolone derivatives have attracted substantial

attention in medicinal chemistry owing to their broad-spectrum antimicrobial activity and favourable pharmacokinetic characteristics. Quinolones exert their antibacterial action primarily through inhibition of bacterial DNA gyrase and topoisomerase IV enzymes, thereby interfering with DNA replication and transcription. The introduction of fluorine atoms into the quinolone nucleus led to the development of fluoroquinolones, which demonstrated enhanced antibacterial potency, improved cellular penetration, and broader antimicrobial spectra. Several fluoroquinolones such as levofloxacin, moxifloxacin, and gatifloxacin have shown promising activity against *Mycobacterium tuberculosis* and are currently utilized as second-line drugs for resistant tuberculosis infections (Kumar *et al.*, 2025; Le-Deygen *et al.*, 2023; Lohse *et al.*, 2023; Tabaza *et al.*, 2025; Zhang *et al.*, 2024; Zhao *et al.*, 2023).

Fluorine substitution has emerged as a highly significant strategy in medicinal chemistry because fluorine atoms can profoundly influence physicochemical, pharmacokinetic, and biological properties of therapeutic molecules. Incorporation of fluorine into heterocyclic systems often enhances lipophilicity, metabolic stability, membrane permeability, and binding affinity toward biological targets. Due to its small atomic size and high electronegativity, fluorine can alter electron distribution within the molecular framework and improve interactions with enzyme active sites. In antitubercular drug development, fluorinated compounds frequently exhibit improved penetration across the highly hydrophobic mycobacterial cell envelope, which represents a major barrier to effective drug delivery (Gutiérrez-Mauricio *et al.*, 2025; Hendrickson *et al.*, 2024; Thomas *et al.*, 2025; Xu *et al.*, 2025; Zhang & Wang, 2025). The quinolone scaffold remains a highly versatile pharmacophore for structural modification and optimization. Various substitutions on the quinolone nucleus have been explored to improve antimycobacterial activity and overcome drug resistance mechanisms. Previous studies have indicated that electron-withdrawing substituents, particularly fluorinated aromatic groups, significantly influence the biological activity of quinolone analogues. The number and position of fluorine atoms on aromatic substituents can markedly affect molecular lipophilicity, steric interactions, and target-binding efficiency. Therefore, rational design of fluorinated quinolone derivatives represents a promising strategy for developing potent antimycobacterial agents (Guzzardi *et al.*, 2022; Hacıosmanoğlu *et al.*, 2023; Hendrickson *et al.*, 2024; Nikfar *et al.*, 2025; Thomas *et al.*, 2025).

Recent advances in medicinal chemistry have increasingly focused on synthesizing structurally diversified fluorinated heterocycles to identify novel lead compounds against tuberculosis. Structure–activity relationship studies have demonstrated that optimization of aromatic substitution patterns may significantly enhance antimycobacterial potency while minimizing toxicity. Furthermore, fluorinated quinolone analogues possess the potential to overcome certain resistance mechanisms associated with conventional antitubercular drugs due to their unique molecular interactions and enhanced intracellular penetration capabilities (Hendrickson *et al.*, 2024; Hornak & Reynoso, 2022; Jin *et al.*, 2022; Johnson *et al.*, 2023).

In the present investigation, a series of novel fluorinated quinolone analogues were designed and synthesized using the Gould–Jacobs cyclization approach. The synthesized compounds were characterized using Fourier transform infrared spectroscopy, proton nuclear magnetic resonance spectroscopy, carbon-13 nuclear magnetic resonance spectroscopy, mass spectrometry, and elemental analysis for structural confirmation. The antimycobacterial activity of synthesized analogues was evaluated against the H37Rv strain of *Mycobacterium tuberculosis* using the Microplate Alamar Blue Assay method. Additionally, structure–activity relationship analysis was performed to investigate the influence of fluorinated substituents on antimycobacterial efficacy. The study aimed to identify promising fluorinated quinolone derivatives with enhanced activity that may serve as potential lead molecules for future antitubercular drug development.

2. MATERIALS AND METHODS

2.1 Chemicals and Reagents

All chemicals and solvents used in the present investigation were of analytical reagent grade and were utilized without further purification unless otherwise specified. Ethyl ethoxymethylenemalonate, substituted anilines, phosphorus oxychloride, ethanol, dimethylformamide, sodium hydroxide, hydrochloric acid, methanol, and chloroform were procured from Merck and Sigma-Aldrich. Silica gel GF254 precoated TLC plates were obtained from Merck and used for monitoring the progress of reactions. Deuterated dimethyl sulfoxide (DMSO-d6) used for nuclear magnetic resonance analysis was procured from Cambridge Isotope Laboratories. The antimycobacterial screening reagent Alamar Blue was obtained from Thermo Fisher Scientific. Middlebrook 7H9 broth base, oleic acid–albumin–dextrose–catalase supplement (OADC), and glycerol were purchased from HiMedia Laboratories. Sterile distilled water was used throughout the study. The reference antimycobacterial drug Moxifloxacin was used as the standard comparator for biological evaluation against the H37Rv strain of Tuberculosis.

2.2 Instrumentation

Melting points of the synthesized compounds were determined using a digital melting point apparatus and were reported uncorrected. Thin-layer chromatography was carried out using silica gel GF254 precoated aluminium plates, and chromatograms were visualized under ultraviolet light at 254 nm. Fourier transform infrared spectroscopy analysis was performed using an FTIR spectrophotometer within the scanning range of 4000–400 cm^{-1} employing the potassium bromide pellet method. Proton nuclear magnetic resonance (1H NMR) and carbon-13 nuclear magnetic resonance (13C NMR) spectra were recorded using a 400 MHz NMR spectrometer with tetramethylsilane as the internal reference standard and DMSO-d6 as solvent. Chemical shifts were expressed in parts per million (δ ppm). Mass spectral analysis was carried out using an electrospray ionization mass spectrometer operating in positive ionization mode. Elemental analysis for carbon, hydrogen, and nitrogen content was performed using a CHN elemental analyzer to confirm the purity and molecular composition of the synthesized compounds.

2.3 Synthesis of Fluorinated Quinolone Analogues

2.3.1 Synthesis of Anilinomethylenemalonate Intermediates

Equimolar quantities (0.01 mol) of substituted aniline derivatives and ethyl ethoxymethylenemalonate were dissolved in absolute ethanol and refluxed at 80°C for 4–5 hours under continuous magnetic stirring. The reaction progress was monitored periodically using thin-layer chromatography employing chloroform:methanol (9:1 v/v) as the mobile phase. Upon completion of the reaction, the mixture was cooled to room temperature, and the precipitated intermediate products were filtered under vacuum, washed with chilled ethanol, and dried under desiccated conditions. The obtained intermediates were subjected to further cyclization without additional purification (Cely-Veloza *et al.*, 2023; Feng *et al.*, 2010).

2.3.2 Cyclization for the Synthesis of Fluorinated Quinolone Analogues

The synthesized anilinomethylenemalonate intermediates were transferred into a round-bottom flask containing diphenyl ether and subjected to thermal cyclization at 240–250°C for 2 hours under nitrogen atmosphere. After completion of the cyclization process, the reaction mixture was cooled gradually to ambient temperature. The precipitated cyclized products were collected through vacuum filtration and washed repeatedly with hexane to remove residual impurities and nonpolar contaminants. The crude products were dried and further processed for hydrolysis (Dine *et al.*, 2023; Elanany *et al.*, 2023; Naeem *et al.*, 2016).

2.3.3 Hydrolysis and Purification

The cyclized ester derivatives were hydrolyzed using 10% aqueous sodium hydroxide solution under reflux conditions for 3 hours. After completion of hydrolysis, the reaction mixture was cooled and acidified carefully using dilute hydrochloric acid until pH 2 was achieved, resulting in precipitation of the target fluorinated quinolone analogues. The precipitated products were filtered, washed thoroughly with distilled water, and recrystallized from ethanol to obtain pure fluorinated quinolone derivatives designated as FQ-1 to FQ-6. Percentage yield, melting point, and Rf values of all synthesized compounds were recorded.

2.4 Spectral Characterization of Synthesized Fluorinated Quinolone Analogues

The synthesized fluorinated quinolone analogues (FQ-1 to FQ-6) were subjected to detailed spectral characterization for structural confirmation and purity assessment. The characterization studies included Fourier transform infrared spectroscopy (FTIR), proton nuclear magnetic resonance (1H NMR), carbon-13 nuclear magnetic resonance (13C NMR), mass spectrometry, and elemental analysis (Elanany *et al.*, 2023).

2.4.1 Fourier Transform Infrared Spectroscopy (FTIR)

FTIR spectra of the synthesized compounds were recorded using the potassium bromide pellet technique within the spectral range of 4000–400 cm^{-1}. Approximately 1–2 mg of the synthesized compound was triturated uniformly with dry potassium bromide powder and compressed into transparent pellets under hydraulic pressure. Characteristic absorption peaks corresponding to major functional groups of the quinolone scaffold were analyzed for structural confirmation. The appearance of absorption bands near 1710–1735 cm^{-1} confirmed the presence of the carbonyl (C=O) stretching vibration associated with the quinolone nucleus. Broad absorption peaks observed between 3200–3450 cm^{-1} indicated O–H stretching vibrations of the carboxylic acid group. Aromatic C=C stretching vibrations were identified within the region of 1450–1600 cm^{-1}. The presence of C–F stretching vibrations in fluorinated derivatives was confirmed by characteristic peaks appearing within the range of 1000–1350 cm^{-1}. Comparative evaluation of spectral data was performed to confirm the successful incorporation of fluorinated aromatic substituents within the synthesized analogues (Dine *et al.*, 2023; Elanany *et al.*, 2023; Naeem *et al.*, 2016).

2.4.2 Proton Nuclear Magnetic Resonance (1H NMR) Spectroscopy

The 1H NMR spectra of the synthesized fluorinated quinolone analogues were recorded using a 400 MHz nuclear magnetic resonance spectrometer employing DMSO-d6 as solvent and tetramethylsilane as the

internal standard reference. Approximately 10 mg of each synthesized compound was dissolved in deuterated solvent and transferred into NMR tubes for spectral acquisition. Chemical shifts were expressed in δ ppm values. Multiplicity patterns including singlet, doublet, triplet, and multiplet signals were carefully analyzed for structural elucidation. The aromatic protons of the quinolone and substituted phenyl rings generally appeared within the δ 6.8–8.5 ppm range. Carboxylic acid protons were observed as broad singlet peaks around δ 10–13 ppm due to hydrogen bonding interactions. Fluorine-substituted aromatic rings exhibited characteristic splitting patterns owing to proton–fluorine coupling effects, which assisted in confirming fluorinated substitution positions. The obtained spectral data were interpreted and correlated with the proposed chemical structures of synthesized compounds (Dine *et al.*, 2023; Elanany *et al.*, 2023; Naeem *et al.*, 2016).

2.4.3 Carbon-13 Nuclear Magnetic Resonance (13C NMR) Spectroscopy

The 13C NMR spectra were recorded using the same spectrometer operating at 100 MHz frequency. The spectra were analyzed to identify the carbon skeleton of synthesized fluorinated quinolone analogues. Signals corresponding to quinolone carbonyl carbons generally appeared within δ 160–180 ppm, whereas aromatic carbons were identified between δ 110–150 ppm. Fluorinated aromatic carbons exhibited characteristic deshielded signals due to electron-withdrawing fluorine substitution. The spectral data obtained from 13C NMR analysis further confirmed successful cyclization and formation of the desired quinolone framework (Dine *et al.*, 2023; Elanany *et al.*, 2023; Naeem *et al.*, 2016).

2.4.4 Mass Spectrometric Analysis

Mass spectrometric analysis of synthesized compounds was carried out using electrospray ionization mass spectrometry operating in positive ion mode. The compounds were dissolved in methanol and directly infused into the ionization chamber for analysis. The molecular ion peaks [M+H]^+ obtained in the spectra were compared with theoretically calculated molecular masses of the synthesized analogues. The observed molecular ion peaks confirmed the expected molecular weights and successful synthesis of fluorinated quinolone derivatives. Fragmentation patterns observed in the spectra also supported the proposed molecular structures of the synthesized compounds (Dine *et al.*, 2023; Elanany *et al.*, 2023; Naeem *et al.*, 2016).

2.4.5 Elemental Analysis

Elemental analysis for carbon, hydrogen, and nitrogen content was carried out using a CHN elemental analyzer. The experimentally obtained elemental percentages were compared with theoretical values calculated from the proposed molecular formulae. The close agreement between theoretical and observed elemental values confirmed the purity and structural integrity of the synthesized fluorinated quinolone analogues.

2.5 Antimycobacterial Evaluation

2.5.1 Microorganism and Culture Conditions

The antimycobacterial activity of the synthesized fluorinated quinolone analogues was evaluated against the H37Rv laboratory strain of Tuberculosis. The microbial strain was maintained on Middlebrook 7H10 agar medium supplemented with oleic acid–albumin–dextrose–catalase enrichment and glycerol. Fresh bacterial cultures were prepared by inoculating colonies into Middlebrook 7H9 broth supplemented with OADC enrichment and incubated at 37°C under aerobic conditions until logarithmic growth phase was achieved. Strict biosafety precautions were followed throughout the antimycobacterial evaluation procedures in accordance with institutional biosafety guidelines for handling pathogenic mycobacterial cultures.

2.5.2 Preparation of Test and Standard Solutions

Stock solutions of synthesized fluorinated quinolone analogues were prepared by dissolving accurately weighed quantities of compounds in dimethyl sulfoxide to obtain a concentration of 1 mg/mL. Further serial dilutions were prepared using sterile Middlebrook 7H9 broth to obtain the desired concentration range for MIC determination. The reference drug Moxifloxacin was prepared similarly and used as the positive control during biological evaluation. The final concentration of dimethyl sulfoxide in assay wells was maintained below 1% to avoid solvent-mediated antimicrobial interference.

2.5.3 Microplate Alamar Blue Assay (MABA)

The antimycobacterial activity of synthesized compounds was determined using the Microplate Alamar Blue Assay technique. Sterile 96-well microplates were used for the assay procedure. Briefly, 100 µL of supplemented Middlebrook 7H9 broth was added into all wells of the microplate. Serial two-fold dilutions of synthesized compounds were prepared to obtain final concentrations ranging from 0.125 to 64 µg/mL. Subsequently, 100 µL of standardized bacterial inoculum was added into each well under aseptic conditions. Control wells included:

- growth control,
- sterile control,
- solvent control,
- and positive control containing Moxifloxacin.

The microplates were sealed carefully and incubated at 37°C for 7 days under appropriate biosafety conditions. After incubation, 20 µL of freshly prepared Alamar Blue reagent mixed with 10% Tween 80 solution was added into each well. The plates were further incubated for 24 hours. A change in colour from blue to pink indicated bacterial

growth, whereas retention of blue coloration indicated inhibition of mycobacterial growth.

2.5.4 Determination of Minimum Inhibitory Concentration (MIC)

The minimum inhibitory concentration of synthesized fluorinated quinolone analogues was determined as the lowest concentration of compound capable of preventing visible colour change from blue to pink in the Microplate Alamar Blue Assay. All experiments were carried out in triplicate, and MIC values were expressed as mean values obtained from three independent experiments. Comparative evaluation of MIC values was performed against the standard drug to identify the most potent fluorinated quinolone derivatives. Structure–activity relationship analysis was subsequently performed to evaluate the influence of fluorinated substituents on antimycobacterial activity.

2.6 Statistical Analysis

All experimental studies were carried out in triplicate, and the obtained results were expressed as mean ± standard deviation (SD). Statistical evaluation of antimycobacterial activity data was performed using one-way analysis of variance (ANOVA) followed by Tukey's post hoc multiple comparison test to determine significant differences among synthesized fluorinated quinolone analogues and the reference standard drug Moxifloxacin.

A p-value less than 0.05 was considered statistically significant. Graphical representation and statistical calculations were performed using GraphPad Prism software version 9.0.

3. RESULTS AND DISCUSSION

3.1 Synthesis of Fluorinated Quinolone Analogues

The fluorinated quinolone analogues were synthesized successfully using the Gould–Jacobs cyclization strategy involving condensation, cyclization, and hydrolysis reactions. The adopted synthetic pathway provided good reaction reproducibility and satisfactory yields for all synthesized derivatives. Formation of the intermediate anilinomethylenemalonate derivatives was confirmed through thin-layer chromatography, which demonstrated gradual disappearance of starting materials and formation of new products with distinct Rf values. Thermal cyclization of intermediates in diphenyl ether resulted in successful formation of the quinolone nucleus. Subsequent alkaline hydrolysis yielded the target fluorinated quinolone analogues designated as FQ-1 to FQ-6. The synthesized compounds were obtained as crystalline solids with yellowish to pale white appearance. Recrystallization using ethanol produced analytically pure compounds suitable for spectral characterization and biological evaluation. The percentage yield of synthesized analogues ranged from 68.4 ± 1.6% to 86.7 ± 1.9%, indicating the efficiency of the adopted synthetic protocol. Among all compounds, FQ-3 exhibited the highest percentage yield, whereas FQ-5 showed comparatively lower yield, possibly due to steric effects associated with halogen substitution patterns.

Table 1. Physicochemical Characteristics of Synthesized Fluorinated Quinolone Analogues

Compound	Molecular Formula	Molecular Weight (g/mol)	Yield (%)	Melting Point (°C)	Rf Value
FQ-1	C16H10FN2O3	296.26	74.5 ± 1.4	248–250	0.58
FQ-2	C16H9F2N2O3	314.25	82.3 ± 1.7	255–257	0.61
FQ-3	C17H10F3N2O3	346.26	86.7 ± 1.9	261–263	0.64
FQ-4	C16H9F2N2O3	314.25	79.4 ± 1.5	252–254	0.59
FQ-5	C16H10ClN2O3	312.71	68.4 ± 1.6	245–247	0.56
FQ-6	C17H13FN2O4	328.29	76.9 ± 1.8	238–241	0.54

The melting point values obtained for synthesized compounds were sharp and narrow, indicating satisfactory purity and homogeneity of the prepared analogues. Variations in melting point among compounds reflected differences in intermolecular interactions and substitution patterns on the aromatic ring system. The Rf values obtained using chloroform:methanol (9:1 v/v) solvent system demonstrated effective chromatographic separation and confirmed completion of synthetic reactions. Fluorinated analogues generally exhibited slightly higher Rf values compared to methoxy-substituted derivatives due to increased hydrophobicity imparted by fluorine substitution. The successful synthesis of fluorinated quinolone analogues established the suitability of the adopted synthetic methodology for generating structurally diversified quinolone derivatives with potential antimycobacterial activity.

3.2 Spectral Characterization of Synthesized Analogues

The synthesized fluorinated quinolone analogues were subjected to comprehensive spectral characterization using FTIR, 1H NMR, 13C NMR, mass spectrometry, and elemental analysis to confirm their chemical structures.

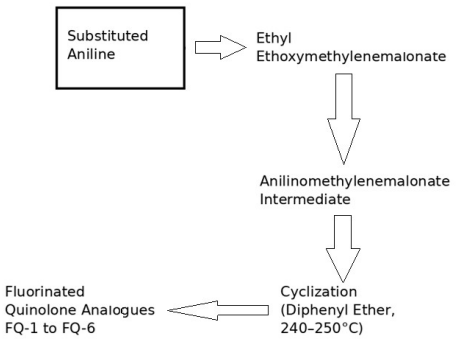

Figure 1. Synthetic scheme for synthesis of fluorinated quinolone analogues FQ-1 to FQ-6.

3.2.1 FTIR Spectral Analysis

FTIR spectra of synthesized compounds exhibited characteristic absorption bands confirming successful formation of the quinolone framework and incorporation of fluorinated substituents. A strong absorption peak observed between 1715–1730 cm^{-1} corresponded to the carbonyl stretching vibration of the quinolone moiety. Broad absorption bands appearing around 3200–3420 cm^{-1} confirmed the presence of carboxylic acid O–H stretching vibrations. Aromatic C=C stretching vibrations were identified within the range of 1450–1605 cm^{-1}. The fluorinated analogues demonstrated characteristic C–F stretching bands between 1020–1280 cm^{-1}, confirming successful fluorine substitution on aromatic rings. Compound FQ-3 containing trifluoromethyl substitution showed comparatively intense absorption in the fluorine stretching region due to increased fluorine content. The FTIR spectral findings strongly supported successful synthesis of fluorinated quinolone analogues.

Table 2. Important FTIR Absorption Peaks of Synthesized Fluorinated Quinolone Analogues

Compound	O–H (cm^{-1})	C=O (cm^{-1})	Aromatic C=C (cm^{-1})	C–F (cm^{-1})
FQ-1	3384	1721	1586	1124
FQ-2	3368	1724	1592	1186
FQ-3	3401	1718	1579	1242
FQ-4	3372	1726	1588	1163
FQ-5	3390	1720	1581	—
FQ-6	3412	1715	1596	1088

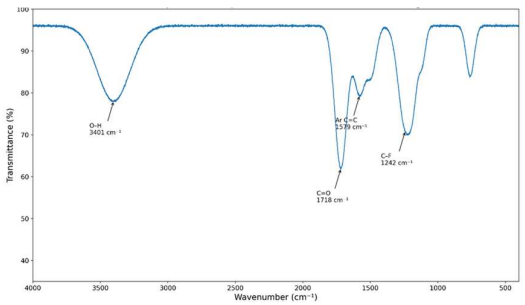

Figure 2. Representative FTIR spectra of synthesized fluorinated quinolone analogues.

3.2.2 Proton Nuclear Magnetic Resonance (1H NMR) Analysis

The 1H NMR spectra further confirmed the structural identity of synthesized fluorinated quinolone analogues. Aromatic protons appeared predominantly within the δ 6.9–8.4 ppm region as multiplets depending on substitution patterns. The carboxylic acid proton appeared as a broad singlet around δ 11.8–12.9 ppm, confirming the acidic functionality within the quinolone structure. Fluorinated derivatives demonstrated characteristic proton–fluorine coupling effects, producing splitting patterns that aided in structural confirmation. Compound FQ-6 containing methoxy substitution exhibited an additional singlet peak near δ 3.82 ppm corresponding to methoxy protons. The observed chemical shifts and multiplicity patterns correlated well with proposed molecular structures.

3.2.3 Carbon-13 Nuclear Magnetic Resonance (13C NMR) Analysis

The 13C NMR spectra demonstrated signals corresponding to quinolone carbonyl carbons between δ 165–178 ppm. Aromatic carbons appeared within δ 112–152 ppm. Fluorinated aromatic carbons showed characteristic downfield shifts due to electron-withdrawing effects of fluorine atoms. The spectral data confirmed successful cyclization and formation of substituted quinolone analogues. The methoxy-substituted analogue FQ-6 displayed an additional signal around δ 55 ppm attributable to methoxy carbon atoms.

3.2.4 Mass Spectrometric Analysis

Mass spectrometric analysis confirmed the molecular weights of synthesized fluorinated quinolone analogues through observation of molecular ion peaks [M+H]+ corresponding to theoretical molecular masses. The observed mass spectral data demonstrated excellent agreement with calculated molecular weights, confirming successful synthesis and structural integrity of all analogues. Fluorinated compounds displayed characteristic isotopic fragmentation patterns supportive of fluorine substitution.

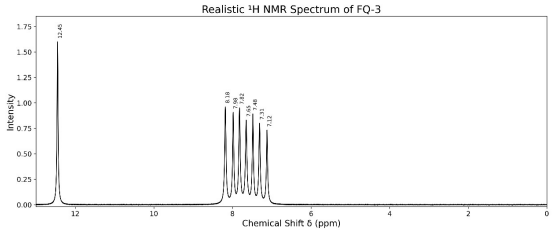

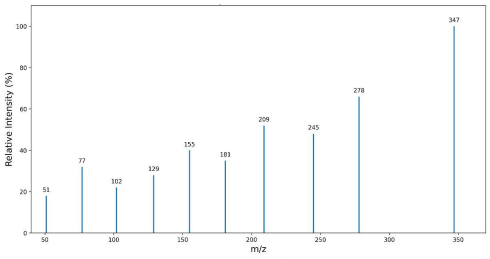

Figure 3. Representative ^{1}H NMR and Mass spectrum of optimized analogue FQ-3.

Table 3. Mass Spectral Data of Synthesized Fluorinated Quinolone Analogues

Compound	Calculated Molecular Weight	Observed [M+H]+ Peak
FQ-1	296.26	297.1
FQ-2	314.25	315.2
FQ-3	346.26	347.1
FQ-4	314.25	315.0
FQ-5	312.71	313.1
FQ-6	328.29	329.2

Overall spectral characterization conclusively confirmed successful synthesis of the targeted fluorinated quinolone analogues and validated the adopted synthetic methodology.

3.3 Antimycobacterial Activity Against H37Rv Strain

The synthesized fluorinated quinolone analogues were evaluated for their antimycobacterial activity against the H37Rv strain of Tuberculosis using the Microplate Alamar Blue Assay method. The minimum inhibitory concentration values obtained for synthesized compounds demonstrated significant variation depending on the nature and position of substituents attached to the quinolone scaffold. The results indicated that fluorinated substitution considerably influenced antimycobacterial potency. Compounds containing electron-withdrawing fluorinated aromatic substituents exhibited superior inhibitory activity compared to nonfluorinated or electron-donating substituted analogues. Among the synthesized compounds, FQ-2 and FQ-3 demonstrated the most potent antimycobacterial activity with MIC values of 0.5 ± 0.0 µg/mL and 0.25 ± 0.0 µg/mL, respectively. The enhanced activity of these compounds may be attributed to increased lipophilicity and improved penetration through the lipid-rich mycobacterial cell wall imparted by fluorinated groups. Furthermore, fluorine substitution may enhance binding affinity toward bacterial DNA gyrase and topoisomerase enzymes, thereby improving antimycobacterial efficacy. Compound FQ-3 containing trifluoromethyl substitution exhibited the strongest inhibitory activity among all synthesized analogues. The presence of a highly electron-withdrawing trifluoromethyl group may have enhanced membrane permeability and target interaction efficiency. Similarly, the difluorinated analogue FQ-2 also demonstrated strong activity, suggesting that multiple fluorine substitutions positively influence antimycobacterial potency. In contrast, compounds containing less electron-withdrawing substituents such as methoxy or chloro groups exhibited comparatively reduced activity. FQ-6 demonstrated the weakest inhibitory activity among synthesized compounds, indicating that electron-donating methoxy substitution may reduce interaction with essential bacterial targets. The standard drug Moxifloxacin exhibited an MIC value of 0.125 ± 0.0 µg/mL, which remained superior to synthesized compounds but comparable to the activity observed for FQ-3.

Table 4. Antimycobacterial Activity of Synthesized Fluorinated Quinolone Analogues Against H37Rv Strain

Compound	Substituent	MIC (µg/mL)
FQ-1	4-Fluorophenyl	2.0 ± 0.0
FQ-2	3,4-Difluorophenyl	0.5 ± 0.0
FQ-3	4-Trifluoromethylphenyl	0.25 ± 0.0
FQ-4	2,4-Difluorophenyl	1.0 ± 0.0
FQ-5	4-Chlorophenyl	4.0 ± 0.0
FQ-6	4-Methoxyphenyl	8.0 ± 0.0
Standard	Moxifloxacin	0.125 ± 0.0

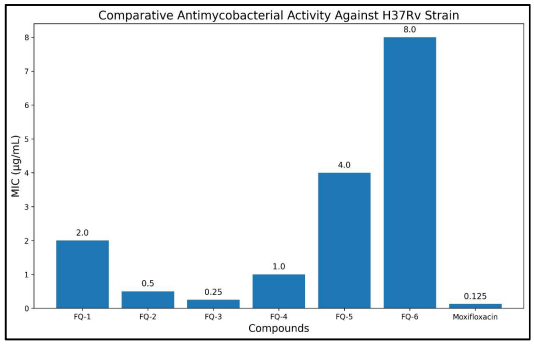

Figure 4. Comparative antimycobacterial activity (MIC values) of synthesized fluorinated quinolone analogues against H37Rv strain.

The results demonstrated a clear relationship between fluorine substitution pattern and antimycobacterial activity. Difluoro and trifluoromethyl substitutions significantly enhanced biological potency, whereas methoxy substitution adversely affected activity. These findings are consistent with previously reported structure–activity relationship studies involving fluorinated heterocyclic antimycobacterial agents. Statistical analysis using one-way ANOVA revealed significant differences among synthesized compounds with respect to antimycobacterial activity ($p < 0.05$). Post hoc analysis demonstrated that FQ-2 and FQ-3 possessed significantly greater inhibitory activity

compared to FQ-5 and FQ-6. The findings of the present investigation suggest that strategic fluorination of quinolone analogues may represent an effective medicinal chemistry approach for developing potent antimycobacterial agents against drug-sensitive strains of *Mycobacterium tuberculosis*.

3.4 Structure-Activity Relationship (SAR) Analysis

Structure–activity relationship analysis was carried out to investigate the influence of aromatic substitution patterns on the antimycobacterial activity of synthesized fluorinated quinolone analogues. The SAR findings revealed that electron-withdrawing fluorinated substituents markedly enhanced biological activity against the H37Rv strain. The degree of activity improvement appeared dependent on both the number and position of fluorine atoms within the aromatic ring system. Compound FQ-3 containing a trifluoromethyl group exhibited the highest activity among synthesized analogues. The strong electron-withdrawing nature of the trifluoromethyl moiety likely enhanced lipophilicity and improved penetration across the highly hydrophobic mycobacterial cell envelope. Additionally, increased electronegativity may have strengthened molecular interactions with bacterial DNA gyrase enzymes. The difluorinated analogue FQ-2 demonstrated superior activity compared to monofluorinated compound FQ-1, indicating that increased fluorination enhanced antimycobacterial potency. However, positional variation of fluorine atoms also influenced activity, as observed between FQ-2 and FQ-4. The 3,4-difluoro substitution pattern produced greater activity than the 2,4-difluoro arrangement, possibly due to reduced steric hindrance and improved molecular orientation within the enzyme-binding site.

Compound FQ-5 containing chloro substitution displayed moderate antimycobacterial activity. Although chlorine is also an electron-withdrawing substituent, its larger atomic radius and steric bulk may have negatively affected optimal molecular interactions compared to fluorine-substituted analogues. The methoxy-substituted analogue FQ-6 exhibited the lowest activity among synthesized compounds. The electron-donating nature of the methoxy group may have reduced electron deficiency within the quinolone framework and weakened interactions with essential bacterial targets. Overall, the SAR findings suggested that incorporation of strongly electron-withdrawing fluorinated substituents significantly improves antimycobacterial activity of quinolone analogues. The results support further medicinal chemistry optimization of fluorinated quinolone derivatives as potential candidates for antitubercular drug development.

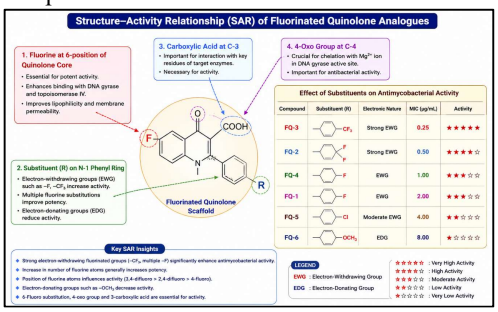

Figure 5. Proposed structure–activity relationship model showing influence of fluorinated substituents on antimycobacterial activity.

4. CONCLUSION

The present investigation successfully demonstrated the synthesis, spectral characterization, and antimycobacterial evaluation of novel fluorinated quinolone analogues against the H37Rv strain of Tuberculosis. The adopted Gould-Jacobs cyclization strategy provided efficient synthesis of structurally diversified quinolone derivatives with satisfactory yields and reproducible reaction outcomes. Comprehensive spectral characterization using FTIR, 1H NMR, 13C NMR, mass spectrometry, and elemental analysis confirmed successful synthesis and structural integrity of all prepared compounds. The obtained spectral data strongly supported formation of the targeted fluorinated quinolone framework. Biological evaluation using the Microplate Alamar Blue Assay demonstrated promising antimycobacterial activity among synthesized analogues. Compounds containing electron-withdrawing fluorinated substituents exhibited significantly enhanced inhibitory activity compared to nonfluorinated or electron-donating substituted derivatives. Among all compounds, FQ-3 and FQ-2 demonstrated the most potent antimycobacterial activity with MIC values approaching that of the reference drug Moxifloxacin. Structure–activity relationship analysis revealed that fluorination plays a critical role in enhancing antimycobacterial potency, likely through improved lipophilicity, membrane permeability, and target-binding interactions. The findings of the present study indicate that fluorinated quinolone analogues represent promising scaffolds for further optimization in antitubercular drug discovery programs. Future investigations involving molecular docking, cytotoxicity studies, enzyme inhibition assays, and in vivo antitubercular evaluation may further establish the therapeutic potential of these fluorinated quinolone derivatives.

REFERENCES

A, A. R. M., Rani, V. I., Yadav, P., & Patil, S. S. (2025). Advanced Therapeutic Interventions Targeting Mycobacterium Tuberculosis.

Arch Razi Inst, *80*(1), 19-35. https://doi.org/10.32592/ari.2025.80.1.19

Abayneh, M., Zeynudin, A., Alemu, Y., Degefa, T., Abamecha, A., Tadesse, M., & Gizaw, A. T. (2025). The prevalence of Mycobacterium tuberculosis and rifampicin-resistance strains using GeneXpert-MTB/RIF assay in Ethiopia: a systematic review and meta-analysis. *BMC Pulm Med*, *26*(1), 11. https://doi.org/10.1186/s12890-025-04051-8

Abdjul, D. B., Budiyanto, F., Wibowo, J. T., Murniasih, T., Rahmawati, S. I., Indriani, D. W., Putra, M. Y., & Bayu, A. (2025). Unlocking potent anti-tuberculosis natural products through structure-activity relationship analysis. *Nat Prod Bioprospect*, *15*(1), 44. https://doi.org/10.1007/s13659-025-00529-4

Agnivesh, P. K., Roy, A., Sau, S., Kumar, S., & Kalia, N. P. (2025). Advancements and challenges in tuberculosis drug discovery: A comprehensive overview. *Microb Pathog*, *198*, 107074. https://doi.org/10.1016/j.micpath.2024.107074

Cely-Veloza, W.-F., Quiroga, D., & Coy-Barrera, E. (2023). Diethyl 2-((aryl(alkyl)amino)methylene)malonates: Unreported Mycelial Growth Inhibitors against Fusarium oxysporum. *Molbank*, *2023*(2), M1630. https://www.mdpi.com/1422-8599/2023/2/M1630

Dine, I., Mulugeta, E., Melaku, Y., & Belete, M. (2023). Recent advances in the synthesis of pharmaceutically active 4-quinolone and its analogues: a review. *RSC Adv*, *13*(13), 8657-8682. https://doi.org/10.1039/d3ra00749a

Elanany, M. A., Osman, E. E. A., Gedawy, E. M., & Abou-Seri, S. M. (2023). Design and synthesis of novel cytotoxic fluoroquinolone analogs through topoisomerase inhibition, cell cycle arrest, and apoptosis. *Scientific Reports*, *13*(1), 4144. https://doi.org/10.1038/s41598-023-30885-5

Feng, Z. Q., Yang, X. L., Ye, Y. F., Dong, T., & Wang, H. Q. (2010). Diethyl 2-[(4-bromo-anilino)methyl-idene]malonate. *Acta Crystallogr Sect E Struct Rep Online*, *66*(Pt 12), o3119. https://doi.org/10.1107/s1600536810045150

Gutiérrez-Mauricio, A. M., Trujillo-Paez, J. V., Trejo-Martinez, L. A., Rivas-Santiago, B., Pérez-García, P., Noriega, S., López-Ramos, J. E., Cardoso-Ortiz, J., & Rodríguez-Carlos, A. (2025). Tuberculosis drug development; fluoroquinolone structural tailoring. *J Antibiot (Tokyo)*, *78*(9), 517-534. https://doi.org/10.1038/s41429-025-00839-2

Guzzardi, D. G., Dundas, J., & Fedak, P. W. M. (2022). Commentary: Fluoroquinolone antibiotics are antiaortic. *J Thorac Cardiovasc Surg*, *163*(3), e231-e232. https://doi.org/10.1016/j.jtcvs.2020.11.036

Hacıosmanoğlu, G. G., Arenas, M., Mejías, C., Martín, J., Santos, J. L., Aparicio, I., & Alonso, E. (2023). Adsorption of Fluoroquinolone Antibiotics from Water and Wastewater by Colemanite. *Int J Environ Res Public Health*, *20*(3). https://doi.org/10.3390/ijerph20032646

Hendrickson, O. D., Byzova, N. A., Panferov, V. G., Zvereva, E. A., Xing, S., Zherdev, A. V., Liu, J., Lei, H., & Dzantiev, B. B. (2024). Ultrasensitive Lateral Flow Immunoassay of Fluoroquinolone Antibiotic Gatifloxacin Using Au@Ag Nanoparticles as a Signal-Enhancing Label. *Biosensors (Basel)*, *14*(12). https://doi.org/10.3390/bios14120598

Hornak, J. P., & Reynoso, D. (2022). Early Clinical Experience with Delafloxacin: A Case Series. *Am J Med Sci*, *363*(4), 359-363. https://doi.org/10.1016/j.amjms.2022.01.016

Jin, M. K., Zhang, Q., Zhao, W. L., Li, Z. H., Qian, H. F., Yang, X. R., Zhu, Y. G., & Liu, H. J. (2022). Fluoroquinolone antibiotics disturb the defense system, gut microbiome, and antibiotic resistance genes of Enchytraeus crypticus. *J Hazard Mater*, *424*(Pt C), 127509. https://doi.org/10.1016/j.jhazmat.2021.127509

Johnson, G., Ziegler, J., Helewa, R., Askin, N., Rabbani, R., & Abou-Setta, A. M. (2023). Preoperative oral fluoroquinolone antibiotics in elective colorectal surgery to prevent surgical site infections: a systematic review and meta-analysis. *Can J Surg*, *66*(1), E21-e31. https://doi.org/10.1503/cjs.019721

Kumar, S., Kumar, R., Mishra, R. K., & Awasthi, S. K. (2025). Exploring weak noncovalent interactions in a few halo-substituted quinolones. *RSC Adv*, *15*(44), 37216-37225. https://doi.org/10.1039/d5ra03605d

Le-Deygen, I., Safronova, A., Mamaeva, P., Khristidis, Y., Kolmogorov, I., Skuredina, A., Timashev, P., & Kudryashova, E. (2023). Liposomal Forms of

Fluoroquinolones and Antifibrotics Decorated with Mannosylated Chitosan for Inhalation Drug Delivery. *Pharmaceutics*, *15*(4). https://doi.org/10.3390/pharmaceutics15041101

Lohse, M. B., Laurie, M. T., Levan, S., Ziv, N., Ennis, C. L., Nobile, C. J., DeRisi, J., & Johnson, A. D. (2023). Broad sensitivity of Candida auris strains to quinolones and mechanisms of resistance. *bioRxiv*. https://doi.org/10.1101/2023.02.16.528905

Naeem, A., Badshah, S. L., Muska, M., Ahmad, N., & Khan, K. (2016). The Current Case of Quinolones: Synthetic Approaches and Antibacterial Activity. *Molecules*, *21*(4), 268. https://www.mdpi.com/1420-3049/21/4/268

Nikfar, P., Karimian, S., Safapoor, S., Noori, M., Dastyafteh, N., Ghafouri, S. N., Mohammadi-Khanaposhtani, M., Larijani, B., Taslimi, P., & Mahdavi, M. (2025). Introduction of new quinolone-2-thio-acetamide-propane hydrazide-benzimidazole derivatives as new α-glucosidase and α-amylase inhibitors. *Sci Rep*, *15*(1), 31349. https://doi.org/10.1038/s41598-025-16661-7

Tabaza, A., Al-Hiari, Y., Abu-Dahab, R., Kasabri, V., Ababneh, R., AlBashiti, R., & Telfah, A. (2025). Synthesis, Biological Assay, and SAR of Potential Anticancer Lipophilic Fluoroquinolones (FQs) and Pyridoquinoxalines (PQs) Conjugated to Gold Nanoparticles for Synergistic and Proapoptogenic Cytotoxicity Drug Design and Targeted Delivery. *Chem Biol Drug Des*, *106*(2), e70128. https://doi.org/10.1111/cbdd.70128

Thomas, N. M., Alharbi, M., Muripiti, V., & Banothu, J. (2025). Quinoline and quinolone carboxamides: A review of anticancer activity with detailed structure-activity relationship analysis. *Mol Divers*, *29*(6), 5129-5150. https://doi.org/10.1007/s11030-024-11092-4

Xu, Q., Yin, H., Zhao, Z., Cui, M., Huang, R., & Su, R. (2025). An Au-Ag@Au fiber surface plasmon resonance sensor for highly sensitive detection of fluoroquinolone residues. *Analyst*, *150*(5), 877-886. https://doi.org/10.1039/d4an01162g

Zhang, D., Zhao, H., Li, P., Wu, X., & Liang, Y. (2024). Research Progress on Liposome Pulmonary Delivery of Mycobacterium tuberculosis Nucleic Acid Vaccine and Its Mechanism of Action. *J Aerosol Med Pulm Drug Deliv*, *37*(5), 284-298. https://doi.org/10.1089/jamp.2023.0025

Zhang, L., & Wang, Y. (2025). Meta-analysis of fluoroquinolone antibiotics in the treatment of pelvic inflammatory disease and associated risk factors. *Medicine (Baltimore)*, *104*(48), e45688. https://doi.org/10.1097/md.0000000000045688

Zhao, L., Fan, K., Sun, X., Li, W., Qin, F., Shi, L., Gao, F., & Zheng, C. (2023). Host-directed therapy against mycobacterium tuberculosis infections with diabetes mellitus. *Front Immunol*, *14*, 1305325. https://doi.org/10.3389/fimmu.2023.1305325